

CROSS SECTION FOR THE  $^{165}\text{Ho}(n, 2n)^{164}\text{Ho}$   
REACTION AT 15.6 MeV

APPROVED:

Pat M. Windham  
Major Professor

David R. Cecil  
Minor Professor

L. J. Bonnell  
Director of the Department of Physics

Robert B. Toulouse  
Dean of the Graduate School

CROSS SECTION FOR THE  $^{165}\text{Ho}(n, 2n)^{164}\text{Ho}$   
REACTION AT 15.6 MeV

THESIS

Presented to the Graduate Council of the  
North Texas State University in Partial  
Fulfillment of the Requirements

For the Degree of

MASTER OF SCIENCE

BY

Richard D. Lear, B.S.

Denton, Texas

August, 1969

TABLE OF CONTENTS

	Page
LIST OF TABLES . . . . .	iv
LIST OF ILLUSTRATIONS . . . . .	v
Chapter	
I. INTRODUCTION . . . . .	1
II. SAMPLE PREPARATION AND ACTIVATION . . . . .	4
III. GAMMA-RAY ENERGY SPECTRUM ANALYSIS . . . . .	6
IV. PROCEDURES FOR ANALYSIS OF DATA . . . . .	10
V. CONCLUSION . . . . .	22
APPENDIX A . . . . .	25
APPENDIX B . . . . .	29
FOOTNOTES . . . . .	37
BIBLIOGRAPHY . . . . .	39

LIST OF TABLES

Table	Page
I. Q Values for Reaction in $^{141}\text{Pr}$ Induced by Fast Neutrons . . . . .	26
II. $^{141}\text{Pr}(n, 2n)^{140}\text{Pr}$ Cross Section. . . . .	27
III. Terms Used in Data Analysis. . . . .	28

## LIST OF ILLUSTRATIONS

Figure	Page
1. Decay Scheme for $^{164}\text{Ho}$ . . . . .	30
2. Half-life Plot for $^{164}\text{Ho}$ . . . . .	31
3. Decay Scheme for $^{140}\text{Pr}$ . . . . .	32
4. Energy Calibration Spectrum . . . . .	33
5. Source Positioning Jig . . . . .	34
6. Activation Spectrum of $^{164}\text{Ho}$ and $^{140}\text{Pr}$ . . . . .	35
7. Relative Efficiency vs Energy Curves for Ge(Li) Detector . . . . .	36

## CHAPTER I

### INTRODUCTION

It was the purpose of this investigation to bring together the ideas and procedures involved in the measurement of (n, 2n) reaction cross sections. Such measurements cannot be made directly, but may be inferred by radioactivity produced by the reaction. In the measurement of this activity and the determination of its relationship to the cross section, it becomes apparent that some of the intrinsic properties of the equipment must be evaluated. Some of the inherent properties of the material under investigation are also involved in determining these relationships. These properties must be determined by the experimenter or accepted from the literature. The following is a discussion of how these properties may be evaluated and related to the reaction cross section for (n, 2n) reactions.

Holmium is a suitable choice for this experiment since only four values of the total  $^{165}\text{Ho}(n, 2n)^{164}\text{Ho}$  cross section have been reported. These measurements indicate the cross section to be between 1750 and 2800 mb for incident neutron energies between 14 and 15 MeV. Khurana and Hans<sup>1</sup> report 2760±210 mb at 14.8 MeV. Bonazzola et al.<sup>2</sup> report 2760±55 mb at 14.7 MeV. Sethi and Mukherjee<sup>3</sup> report 1780±140 mb at 14 MeV.

Menlove et al.<sup>4</sup> have reported an excitation function for this cross section which is normalized to the value by Sethi and Mukherjee.

Brown and Becker<sup>5</sup> reported an examination of the decay of  $^{164}\text{Ho}$  in 1954. They proposed a decay scheme and reported the possible existence of a metastable state in  $^{164}\text{Ho}$ . This article was followed in 1966 with a further investigation by Jorgensen et al.<sup>6</sup> and Sethi and Mukherjee.<sup>3</sup> Both papers confirm the existence of the metastable state in  $^{164}\text{Ho}$ . They both propose the same decay scheme, which is shown in Figure 1. The confirmation of the metastable state is made by observing the 91.3-KeV gamma ray from  $^{164}\text{Er}$  and the 73-KeV gamma ray from  $^{164}\text{Dy}$  with a NaI detector. These gamma rays give the half life of the ground state. The half life of the metastable state is observed through the 37-KeV gamma ray. Jorgensen et al. report a 29-minute half life for the ground state while they observe a 37.5-minute half life for the metastable state. Sethi and Mukherjee report a similar finding, showing a  $39.0 \pm 0.5$  minute half life for metastable state and a  $23.9 \pm 0.5$  minute half life for the ground state. The procedure outlined above was repeated in this experiment using a Ge(Li) detector. A single-channel analyzer was set up to bracket the 91.3 and 73-KeV photo-peaks. The output of the single-channel analyzer was used

to drive a scaler. A half-life measurement was made on the above two peaks simultaneously. No separate half life for the ground state was observed. Figure 2 shows the half-life curve obtained in this experiment. Sethi and Mukherjee attempted some coincidence work to support further the existence of the metastable state. It appears from their published coincidence spectra that their arguments are weakened by the lack of resolution from the NaI crystal and the lack of good statistics in the reported coincidence spectra.

A search of the literature was also made to determine the branching ratios for the decay of the ground state of  $^{164}\text{Ho}$ . The branching ratio to the 91.3-KeV level in  $^{164}\text{Er}$  was needed for the calculations made in this experiment. Three values were found for this branching ratio. The Nuclear Data Sheets<sup>7</sup> gives 8%, Brown and Becker report 15% and Sethi and Mukherjee report 22%.



## CHAPTER II

### SAMPLE PREPARATION AND ACTIVATION

Holmium and praseodymium samples were obtained from Alpha Inorganic in the form of foils having a thickness of 0.005 inches and a chemical purity of 99.99%. The Pr was used as a neutron-flux monitor. Activation samples were prepared by cutting disks of 3/4-inch diameter from these foils. The Pr oxidized readily in air and thus had to be coated with the material which would prevent contact with the air. Lacquer was chosen for this coating because of the ease of application. An analysis was performed to ascertain whether the lacquer would make a contribution to the gamma-ray energy spectrum. A sample of Pr was prepared in an atmosphere of He and encapsulated in a neoprene rabbit for which the spectrum was known. An activation was then made on this sample and on one which had been prepared with lacquer. A comparison of these two spectra revealed that no contribution was made by the lacquer. The Ho does not oxidize readily, hence no special protective procedures to insure against source deterioration were necessary. To complete the fabrication of the activation sample, after the Pr was sprayed with lacquer, the Ho and Pr were pressed together and allowed to dry as a unit, being bound by the lacquer.

Thus an activation sample consisted of a "sandwich" of one disk of Ho and one disk of Pr.

The Regional Nuclear Physics Laboratory's<sup>8</sup> 2MV Van de Graaff accelerator was used to provide the neutron fluxes for this work. The  ${}^3\text{T}(\text{D},\text{n}){}^4\text{He}$  reaction at a bombarding energy of  $550\pm 50$  KeV was used as the source of neutrons. At this deuteron energy, the neutron energy at  $0^\circ$  is 15.9 MeV.<sup>9</sup> The sample subtended an angle from  $0^\circ$  to  $46^\circ$ . Thus the neutron energy varied from 15.9 MeV to 15.4 MeV with the weighted average energy being 15.6 MeV.

The activation sample and the neutron flux monitor were prepared with the same geometrical dimensions in order to eliminate the calculation of complicated geometrical factors, which appear in the equations used to relate the gamma-ray energy spectrum to the cross section. Because the samples were so thin, the flux experienced by the foil facing the neutron target and the flux experienced by the second foil were the same. To verify the accuracy of this assumption, activations were made with the Pr disk facing the neutron flux and with the Ho disk facing the neutron flux. Cross-section measurements showed that the same results were obtained with either orientation, which means that the flux will cancel out of the final equation used for cross-section calculation. These points are consistent with the results of calculations utilizing the mathematical equations developed in a later chapter.

## CHAPTER III

### GAMMA-RAY ENERGY SPECTRUM ANALYSIS

The gamma-ray energy spectra were recorded using a 2-cm<sup>3</sup> planar Ge(Li) detector which has a resolution of 4.8 KeV at 511 KeV. The detector was used in conjunction with a Tennelec TC200 Amplifier-preamplifier system and a 1024-channel Nuclear Data multichannel analyzer.

Figure 1 shows the reported decay scheme for <sup>164</sup>Ho. This decay scheme is under study, as will be discussed in the conclusion. Based upon this decay scheme the radiation which would be detected from the decay of <sup>164</sup>Ho are the following gamma rays: 45.9, 56.1 and 37.0 KeV from the decay of the metastable state of <sup>164</sup>Ho, 91.3 KeV from the decay of <sup>164</sup>Er which is produced when <sup>164</sup>Ho undergoes  $\beta^-$  emission, and 73.0 KeV from the decay of <sup>164</sup>Dy which is produced when <sup>164</sup>Ho undergoes electron capture, as reported by Brown and Becker.<sup>5</sup> Since <sup>164</sup>Dy is created by electron capture there should be K <sub>$\alpha$</sub>  and K <sub>$\beta$</sub>  x-rays emitted. The K <sub>$\alpha$</sub>  x-ray from <sup>164</sup>Dy has an energy of 45.59 KeV and the K <sub>$\beta$</sub>  has an energy of 53.64 KeV.<sup>11</sup> The internal conversion coefficient for the 73 KeV gamma ray in <sup>164</sup>Dy is 8.79.<sup>12</sup> The internal conversion coefficient for the 91.3 KeV gamma ray in <sup>164</sup>Er is 4.63.<sup>12</sup> The K <sub>$\alpha$</sub>  x-ray from <sup>164</sup>Er is 45.65 KeV and the K <sub>$\beta$</sub>  x-ray is 56.35 KeV.<sup>11</sup> Since resolution

of the detector is 4.8 KeV, these x-rays will be inseparable from the 45.9 and 56.1 KeV gamma rays given in the decay scheme. Thus the proposed 45.9 gamma ray from  $^{164m}\text{Ho}$ , the 45.59 KeV  $K_{\alpha}$  x-ray from  $^{164}\text{Dy}$  and the 45.65 KeV  $K_{\alpha}$  x-ray from  $^{164}\text{Er}$  will all appear as one photopeak in the gamma ray spectra. Similarly the proposed 6.1 KeV gamma ray from  $^{164m}\text{Ho}$ , the 53.64 KeV  $K_{\beta}$  x-ray from  $^{164}\text{Dy}$  and the 56.35  $K_{\beta}$  x-ray from  $^{164}\text{Er}$  will all appear as one photopeak in the gamma-ray energy spectrum. When analyzing the gamma-ray energy spectrum, the internal conversion coefficients must be used to account for part of the intensity of the photopeaks at 45.9 and 56.1 KeV. A further explanation follows in Chapter IV.

Figure 3 shows the decay scheme for  $^{140}\text{Pr}$ .<sup>13</sup> This isotope decays 100% to the ground state of  $^{140}\text{Ce}$ . The decay scheme goes 53% by electron capture and 47% by  $\beta^+$  emission. The radiation from this decay which will be detected by the Ge(Li) detector will be the 511-KeV radiation from the annihilation of the  $\beta^+$  particles. Thus the energy spectrum of the combined samples of Ho and Pr will be from 37 to 511 KeV.

The analyzer was calibrated using  $^{133}\text{Ba}$  and  $^{22}\text{Na}$ . The gain settings were set so that the 511-KeV annihilation radiation from  $^{22}\text{Na}$  would fall in the upper channels. The gamma rays from the  $^{133}\text{Ba}$  were used to get an energy calibration for the analyzer. The energy calibration curve is shown in Figure 4.

In order to eliminate the calculation of geometry factors from the equations used to give the cross section, each sample must have the same sample-detector geometry. To insure that the geometry was reproducible, an aluminum jig was made which would hold each sample in the same position on the aluminum vacuum can of the detector with a parallel disk geometry. Figure 5 illustrates this jig. This jig also insured that all of the  $\beta^+$  particles from the decay of  $^{140}\text{Pr}$  annihilate in the vicinity of the sample.

Figure 6 shows a typical spectrum taken from an activated sample. The four lower peaks are the 46.1, 53.0, 73.6, and 90.6 KeV photopeaks from  $^{164}\text{Ho}$  as given by the data taken in this investigation. The higher-energy peak is the 511 KeV photopeak from the annihilation radiation from  $^{140}\text{Pr}$ . The detector used to make the cross-section measurement did not detect the 37 KeV gamma ray from  $^{164}\text{Ho}$ . The absence of this photopeak is due to its low intensity and also because of the thick dead layer on the surface of the detector. The  $0.5 \text{ mm}^{14}$  dead layer traps out the 37 KeV gamma rays before they reach the sensitive volume of the detector. A later spectrum taken with a detector having a thinner dead layer<sup>15</sup> shows the presence of a 37 KeV gamma ray with an intensity six times lower than the 90.6 KeV gamma ray. However, the relative intensity between the 37 KeV and 46.1 KeV gamma rays as reported by Sethi and Mukherjee is higher than the initial measurements of this work. Further work is planned to obtain a better measure-

ment of this photopeak ratio and to attempt to determine whether or not it originates from the  $^{164}\text{Ho}$ .

## CHAPTER IV

### PROCEDURES FOR ANALYSIS OF DATA

The total number of disintegrations during the counting interval is just the number of radioactive nuclei present in the sample when the counting started minus the number existing when the counting is finished. This number (N) is given by the following formula:

$$N = N_a (e^{-\lambda t_1} - e^{-\lambda t_2})$$

where  $\lambda$  is the decay constant for the radioactive isotope produced;  $N_a$  is the total number of active nuclei at the end of the activation process;  $t_1$  is the time lapse between the end of the activation process and the start of the counting, that is, transfer time; and  $t_2$  is the time at which the counting is stopped relative to the end of the activation. A value of N may be calculated from the gamma-ray counts detected during the counting interval, and then by means of the above equation related to the total number of nuclei which were active at the end of the activation process.

A procedure will now be detailed to relate the number of gamma-rays counted during the time  $t_1$  to  $t_2$  to the total number which were emitted during this time interval. Geometry and efficiency correction factors must be included in the

calculations to accomplish this. The geometry factors account for the fact that the detector does not subtend a complete  $4\pi$  solid angle with respect to the source, and will be combined into a constant (G) representing the fraction of the total gamma rays emitted which actually intercept the detector. Once the gamma ray has entered the detector, consideration must be given to how efficiently it can be detected. Because the energies involved in this experiment are below the threshold for pair production, pair production is not possible as one of the interactions of the gamma rays with the detector. The basic mechanisms for interactions are due to Compton scattering and a photoelectric interaction. Since Compton scattering events are displayed in the spectra with a distribution in energy, the only events which will be of importance for determining  $N_a$  will be the photoelectric encounters.

The number of counts under the photopeaks can be related to the number of active nuclei at the end of the activation as follows. Let  $f$  represent that fraction of the gamma rays entering the crystal which undergo a photoelectric interaction. Using these two factors,  $f$  and  $G$ , a relationship can be written which relates the number of gamma rays entering the photopeaks to the actual number emitted as

$$N_c = NfG \quad ,$$



where  $N_c$  = number counted;  $G$  = the fraction of the total gamma rays emitted which actually intercept the detector; and  $N$  = the total number of nuclei decaying during the counting interval. This can in turn be related to the number of active nuclei at the end of the activation process by

$$N_c = fGN_a (e^{-\lambda t_1} - e^{-\lambda t_2}) \quad .$$

According to the proposed decay scheme,  $^{164}\text{Ho}$  decays by  $\beta^-$  emission to  $^{164}\text{Er}$  and by electrons capture to  $^{164}\text{Dy}$ . Because in each case the decay goes partially to the ground state of the residual nuclei with no gamma ray being emitted, it is not possible to account for all of the transitions by summing under the 90.6 and the 73 KeV photopeaks. Hence this technique would not account for the amount of the  $^{164}\text{Ho}$  which decays directly to the ground states of  $^{164}\text{Er}$  and  $^{164}\text{Dy}$ . Using an average of the branching ratios given in Chapter I, the number counted under the 90.6 KeV photopeak can be related to the total number of transitions counted in the counting interval as  $N_{cp} = BN_c$ , where  $N_{cp}$  is the number counted under one photopeak and  $B$  is the branching ratio. Incorporating these relations into the preceding equation gives

$$N_{cp} = BfGN_a (e^{-\lambda t_1} - e^{-\lambda t_2}) \quad .$$

In the above analysis, it has been assumed that all of the transitions at the energy of interest take place by gamma-ray emission. Actually some of the transitions proceed by internal electron conversion. Typically, the electron conversion coefficient ( $\alpha$ ) is defined as the number of conversion electrons divided by the number of gamma rays associated with a certain transition. A factor of  $(1 + \alpha)$  must then be included in the calculations to account for these conversion electrons. Here  $\alpha$  is the electron conversion coefficient for the energy of interest. Thus the equation which relates the number of counts under one gamma-ray photopeak to the actual number of nuclei activated at the end of the activation process becomes

$$(1 + \alpha)N_{cp} = BfGN_a(e^{-\lambda t_1} - e^{-\lambda t_2})$$

or

$$N_a = \frac{N_{cp}(1 + \alpha)}{BfG(e^{-\lambda t_1} - e^{-\lambda t_2})}$$

This equation gives the number of active nuclei at the end of the activation period as a function of the number of nuclei which undergo gamma-ray emission plus the number which are internally converted.

The theories of activation analysis<sup>16</sup> give that

$$I = N_o \sigma \phi (1 - e^{-\lambda t_i}) \quad ,$$

where  $I$  is the intensity at the time the activation is stopped;  $N_0$  is the number of nuclei in the sample;  $\sigma$  is the cross section of the reaction in progress;  $\phi$  is the beam flux;  $\lambda$  is the decay constant; and  $t_i$  is the irradiation time. The intensity at the instant the irradiation process is stopped is given by  $N_a \lambda$ . Thus

$$I = N_a \lambda = N_0 \sigma \phi (1 - e^{-\lambda t_i})$$

As previously stated, the experiment was performed using a sandwich of two thin disks, so that both disks experienced the same flux. A ratio of the equation for the Ho sample with that of the Pr monitor shows that, since the flux was the same for both disks, the flux will cancel out of the equation. Then the ratio of these two equations becomes

$$\frac{\frac{dN_{\text{Ho}}}{dt}}{\frac{dN_{\text{Pr}}}{dt}} = \frac{\lambda(\text{Ho}) N_a(\text{Ho})}{\lambda(\text{Pr}) N_a(\text{Pr})} = \frac{N_0(\text{Ho}) \sigma(\text{Ho}) (1 - e^{-\lambda(\text{Ho}) t_i})}{N_0(\text{Pr}) \sigma(\text{Pr}) (1 - e^{-\lambda(\text{Pr}) t_i})}$$

The above equation can then be rewritten as

$$\frac{\sigma(\text{Ho})}{\sigma(\text{Pr})} = \frac{\lambda(\text{Ho})}{\lambda(\text{Pr})} \frac{N_a(\text{Ho})}{N_a(\text{Pr})} \frac{N_0(\text{Pr})}{N_0(\text{Ho})} \frac{1 - e^{-\lambda(\text{Pr}) t_i}}{1 - e^{-\lambda(\text{Ho}) t_i}} ;$$

but

$$\frac{N_a(\text{Ho})}{N_a(\text{Pr})} = \frac{G(\text{Pr})}{G(\text{Ho})} \frac{N_{cp}(\text{Ho})}{N_{cp}(\text{Pr})} \frac{B(\text{Pr})}{B(\text{Ho})} \frac{f(\text{Pr})}{f(\text{Ho})} \frac{e^{-\lambda(\text{Pr})t_1} - e^{-\lambda(\text{Pr})t_2}}{e^{-\lambda(\text{Ho})t_1} - e^{-\lambda(\text{Ho})t_2}}$$

$$\times \frac{1 + \alpha(\text{Ho})}{1 + \alpha(\text{Pr})}$$

from the previous development. So

$$\frac{\sigma(\text{Ho})}{\sigma(\text{Pr})} = \frac{\lambda(\text{Ho})}{\lambda(\text{Pr})} \frac{N_{cp}(\text{Ho})}{N_{cp}(\text{Pr})} \frac{B(\text{Pr})}{B(\text{Ho})} \frac{f(\text{Pr})}{f(\text{Ho})} \frac{G(\text{Pr})}{G(\text{Ho})} \frac{N_o(\text{Pr})}{N_o(\text{Ho})}$$

$$\times \frac{1 - e^{-\lambda(\text{Pr})t_1}}{1 - e^{-\lambda(\text{Ho})t_1}} \frac{1 + \alpha(\text{Ho})}{1 + \alpha(\text{Pr})} \frac{e^{-\lambda(\text{Pr})t_1} - e^{-\lambda(\text{Pr})t_2}}{e^{-\lambda(\text{Ho})t_1} - e^{-\lambda(\text{Ho})t_2}}$$

Now

$$\frac{\lambda(\text{Ho})}{\lambda(\text{Pr})} = \frac{0.693/T(\text{Ho})}{0.693/T(\text{Pr})} = \frac{T(\text{Pr})}{T(\text{Ho})}$$

where  $T(\text{Pr})$  is the half life of Pr and  $T(\text{Ho})$  is the half life of Ho. The following equation is used to calculate the number of nuclei in the sample.

$$N_o = \frac{N_A}{A} m$$

where  $N_A$  is Avogadro's Number;  $A$  is the atomic mass; and  $m$  is the mass of the sample. Thus

$$\frac{N_o(\text{Pr})}{N_o(\text{Ho})} = \frac{N_A/141 m(\text{Pr})}{N_A/165 m(\text{Ho})} = \frac{m(\text{Pr})}{M(\text{Ho})} \frac{165}{141}$$

where  $m(\text{Pr})$  is the mass of the Pr sample;  $m(\text{Ho})$  is the mass of the Ho sample; 165 is the atomic mass of Ho; and 141 is the atomic mass of Pr.

All of the above ideas can now be combined to give the ratio of the cross sections in terms of the quantities measured in the experiment and known values from the literature. This equation is

$$\frac{\sigma(\text{Ho})}{\sigma(\text{Pr})} = \frac{T(\text{Pr})}{T(\text{Ho})} \frac{1 + \alpha(\text{Ho})}{1 + \alpha(\text{Pr})} \frac{N_{\text{cp}}(\text{Ho})}{N_{\text{cp}}(\text{Pr})} \frac{B(\text{Pr})}{B(\text{Ho})} \frac{f(\text{Pr})}{f(\text{Ho})} \frac{m(\text{Pr})}{m(\text{Ho})}$$

$$\times \frac{G(\text{Pr})}{G(\text{Ho})} \frac{165}{141} \frac{1 - e^{-\lambda(\text{Pr})t_i}}{1 - e^{-\lambda(\text{Ho})t_i}} \frac{e^{-\lambda(\text{Pr})t_1} - e^{-\lambda(\text{Pr})t_2}}{e^{-\lambda(\text{Ho})t_1} - e^{-\lambda(\text{Ho})t_2}}$$

The measured quantities are  $N_{\text{cp}}$ ,  $G$ ,  $m$ ,  $T(\text{Ho})$ ,  $t_i$ ,  $t_1$ , and  $t_2$ . The half life and thus the decay constant can be either measured or accepted from the literature. The values of the quantities  $B$ , atomic mass,  $T(\text{Pr})$ , and  $\alpha$  were obtained from the literature.

Some of the terms in the last equation require some additional explanation concerning their relationship to this experiment. The term  $G$  appears in the equation to account for the solid angle the detector subtends with the sample. Since the sample and the monitor are the same physical size it appears that the factor  $G$  should be the same for the monitor and the sample. This would mean that since the terms enter the equation

as a ratio they could cancel. However there are two possibilities which must be considered that may prevent these terms from being identical: the range of the  $\beta^+$  particles in the aluminum cap and the nature of the annihilation radiation. The annihilation radiation originates at the point of annihilation of the  $\beta^+$  particles. The size of the sample appears to increase by the amount the  $\beta^+$  particles penetrate into the Al. The average penetration should be the half thickness. The following equation can be used to calculate the half thickness of particles in Al:

$$D_{\frac{1}{2}} = 0.04 \frac{E^{1.14}}{\rho} \text{ cm} \quad , \quad 17$$

where E is the energy of the  $\beta$  particles in MeV and  $\rho$  is the density of the absorbing material in grams per  $\text{cm}^3$ . For the 2.23 MeV  $\beta^+$  emitted in the decay of  $^{140}\text{Pr}$  the half thickness is  $D_{\frac{1}{2}} = 0.037$  cm. This is the average distance a  $\beta^+$  emitted from the surface of the Pr would travel. Those emitted below the surface of the Pr sample will travel a shorter distance into the aluminum. A calculation has been made of the probability of the gamma ray intercepting a detector vs distance from the detector and size of sample for a parallel concentric disk geometry.<sup>18</sup> This calculation shows that an increase of 0.037 cm makes an insignificant change in the geometry factor. Because two photons are emitted at  $180^\circ$ , the probability of

detecting a gamma ray originating from the same place. Thus the factor  $G$  for Pr is twice that for Ho.

The efficiency of gamma ray detection varies with energy for any detector. Because the gamma rays for the  $^{164}\text{Ho}$  are lower in energy than the annihilation radiation from  $^{140}\text{Pr}$ , a factor must be determined which relates the efficiencies at different energies. An analytical calculation of these factors is difficult, because of the geometry of the problem, since it leads to an infinite series of integrals which must be evaluated numerically. Numerical calculations have been made of the photopeak efficiency for a beam of parallel flux incident perpendicularly upon a planar detector.<sup>19</sup> A dead layer of 0.2 mm was chosen, with calculations being made for depletion depths from 2 to 10 mm. All of these calculations revealed that at some energy below 100 KeV the photopeak efficiency reached a maximum and then dropped off because of absorption in the dead layer.

Experimental measurements have also been made, using standard sources of known activity, to determine the efficiency-vs-energy curves for Ge(Li) detectors.<sup>20</sup> The geometry is a point source with a 2-cm<sup>3</sup> planar detector with the source located on the axis of the detector. The dead layer is not listed. The maximum efficiency is indicated to occur at about the 32-KeV x-ray energy of  $^{133}\text{Ba}$ .

The relative efficiency-vs-energy curve for the detector used in this experiment was determined using a source for which the relative intensities of the gamma rays are known. Germanium 77 has many gamma rays in the region from 150 to 560 KeV for which the intensities have been published.<sup>21</sup> Barium 133 has seven gamma rays of known intensity in the range from 80 to 384 KeV.<sup>22</sup> The relative efficiency can be calculated for a given source by integrating under all of the photopeaks in the spectrum separately and normalizing the separate intensities to one peak. By comparing these calculated intensities to the known intensities one arrives at the relative efficiency-vs-energy curve for the detector. Now if the curve obtained from  $^{133}\text{Ba}$  is normalized to the curve obtained from the  $^{77}\text{Ge}$ , the relative efficiency-vs-energy curve is obtained in the range from 80 KeV to 560 KeV. Figure 7 shows the curve obtained in this experiment.

Praseodymium has several desirable qualities which allow it to be used as a monitor. Praseodymium has only one stable isotope,  $^{141}\text{Pr}$ . At the energies involved in this experiment the predominant reaction in Pr is  $^{141}\text{Pr}(n, 2n)^{140}\text{Pr}$ . Table 1 lists the Q values for the competing reactions in Pr. These values predict that all of the competing reactions are possible at the incident neutron energy used in this experiment. An examination of the predominant gamma rays from these competing reactions shows that no contribution is made in the energy range



of interest to this experiment. The half life of  $^{140}\text{Pr}$  is well known at  $3.39 \pm 0.01$  min.<sup>23</sup> This half life makes it suitable to use with samples which have a half life from a few seconds to several minutes. This relatively short half life did present a problem if the flux did not remain constant. The activation runs were from 20 minutes to 1 hour in length. The neutron flux measured by the Pr monitor was the flux it experienced the last few minutes of the activation process due to its relatively short half life. If a fluctuation is observed in the neutron flux a correction must be made to relate the average neutron flux the Ho experienced to the neutron flux at the end of the activation process, which is given by the Pr. The fluctuations observed were due to an overall drift in the magnitude of the deuteron beam current. Since the neutron flux is related linearly to the beam current, the correction is just the ratio of the flux at the end of the activation process to the average flux during the process. The  $^{141}\text{Pr}(n, 2n)^{140}\text{Pr}$  cross section has been measured by five different observers. The results are given in Table II. The value used in this experiment is an average of these values weighted by their errors.

The half life of  $^{164}\text{Ho}$  produced in the reaction  $^{165}\text{Ho}(n, 2n)^{164}\text{Ho}$  was measured experimentally. Thirty-second counts were taken with a thirty-second delay between counts. The background was subtracted and an exponential curve was fitted

to the data using the computer least-squares program, EXPO. The results of this analysis give the half life of  $^{164}\text{Ho}$  to be  $40.8 \pm 0.4$  min. The Chi-square test gives a 50% reproducibility factor within the errors quoted. A plot of the half-life data is shown in Figure 1.

As mentioned in the introduction, there has been a diversity of values reported in the literature for the branching ratios. As was mentioned before there is some further work indicated on the decay scheme of  $^{164}\text{Ho}$ . The justification for this work involves questions about the metastable state and not the decay of the ground state  $^{164}\text{Ho}$ . For this reason the branching ratios are valid for this work despite the fact that further work is needed on the decay scheme.

To facilitate the subtraction of background, each spectrum was plotted in the regions of the 90.6 KeV and the 511 KeV photopeaks. The background under the peaks was approximated by a straight line determined by the background level on each side of the peak. The values given by this line were then used to determine the total background under the peak. The error involved in the background subtraction was estimated by considering the maximum possible deviation of the background from the value chosen. It was determined that the error was about 2%.

Table III lists the values of the terms used in this investigation.

## CHAPTER V

### CONCLUSION

The results of this investigation give the value of the total  $^{165}\text{Ho}(n, 2n)^{164}\text{Ho}$  cross section to be  $2000 \pm 960$  mb. This is obviously in the range of values quoted in the introduction. The work reported by Menlove et al. shows the excitation function to be flat between 14 and 16 MeV; hence all of the previous values should be valid at the 15.6 MeV neutron energy of this experiment. A theoretical calculation by Pearlstein<sup>23</sup> shows this cross section to be 2108 mb.

As a further check, the cross-section measurement was repeated using a Cu foil as a monitor. Results of these calculations revealed the (n, 2n) cross section for  $^{165}\text{Ho}$  to be  $2150 \pm 1032$  mb. The data for this part of the experiment were analyzed with the equations previously discussed. The quantities evaluated for Pr were replaced by the appropriate quantities evaluated for Cu. The mass of the Cu foils was greater than that of the Pr foils. The Cu foils also gave gamma rays of energy 2.3, 2.05, and 1.172 MeV. This fact added greatly to the background under the Ho spectrum, because of the added counts due to Compton scattering. The resulting increased background made the statistics of the photopeaks in the Ho spectrum poor because the counts were not sufficiently greater than the background. For this reason the measurements made with the Pr

monitors are believed to be the most accurate.

From the above findings it can be concluded that Pr is not only adequate as a monitor, but is desirable when the activity of the sample under investigation is small. Praseodymium does oxidize rather easily. It must be stored under oil when not in use. However, this inconvenience does not limit the usefulness of Pr as a monitor.

As was stated before, the work done in this experiment indicates further investigation of the decay scheme for  $^{164}\text{Ho}$  is justified. The resolution of the Ge(Li) detector is sufficient to resolve the  $^{164}\text{Ho}$  spectrum into its separate photopeaks. Using this detector a coincidence spectrum can be taken which will resolve the 37 and 46.1 KeV photopeaks. A series of coincidence spectra with this resolution will permit a determination of the origin of the 37 KeV gamma ray. This will aid in substantiating or disproving the existence of the metastable state in  $^{164}\text{Ho}$ .

A half-life measurement of  $^{164}\text{Ho}$  by detecting the  $\beta^-$  particles emitted is planned for the future. This work will be done using a silicon surface-barrier detector. Previous workers have substantiated the existence of the metastable state in  $^{164}\text{Ho}$  by the half-life curve obtained from the  $\beta^-$  emission. The ground state and the metastable state of  $^{164}\text{Ho}$  exist as a mother-daughter decay with the metastable state feeding the ground state. This relationship makes the decay

curve obtained from the  $\beta^-$  particles depart from the decay curve of a simple nuclei. This experiment will also help in substantiating or disproving the existence of the metastable state in  $^{164}\text{Ho}$ .

The values cited in the introduction justify additional work on the branching ratios for  $^{164}\text{Ho}$ . The large error quoted for the measured cross section is due mainly to the uncertainty in the branching ratios. If there were no uncertainty in the branching ratios, the measured cross section value would be  $2000 \pm 100$  mb.

Further work is planned to determine the efficiency as a function of energy for the detectors. These plans include repeating the measured efficiency-vs-energy experiment using  $^{166}\text{Ho}$ . This isotope has many more gamma rays within the range of interest. It also has sufficient gamma rays between 0.5 MeV and 2 MeV. Projected plans concerning the efficiency vs energy of the detector involve work on a theoretical computer program for calculating this curve from the properties of the detector. This work will take into account such factors as absorption in the dead layer, probability of making a photoelectric encounter in the intrinsic volume of the detector, and solid-angle considerations between the sample and the detector.

APPENDIX A

TABLE I

Q VALUES FOR REACTION IN  $^{141}\text{Pr}$  INDUCED BY FAST  
 NUETRONS, ( L. A. KOENIG, J. H. E. MATTAUCH  
 AND A. H. WAPSTRA, (COMPS.), NUCLEAR  
DATA TABLES, PART 2, (1960) )

Outgoing Particles	Residual Nucleus	Q Value (KeV)	Error (KeV)
p	$^{141}\text{Ce}$	202	5
$^2\text{D}$	$^{140}\text{Ce}$	-3102	26
$^3\text{T}$	$^{139}\text{Ce}$	-5910	70
$^3\text{He}$	$^{139}\text{La}$	-5620	70
$^4\text{He}$	$^{138}\text{La}$	1680	20
n+p	$^{140}\text{Ce}$	-5326	26
2p	$^{140}\text{La}$	-8317	31
2n	$^{140}\text{Pr}$	-9368	20

TABLE II

$^{141}\text{Pr}(n, 2n)^{140}\text{Pr}$  CROSS SECTION (M. BORMANN,  
(COMP.), NUCL. PHYS. 65, 257 (1965) )

Neutron Energy (MeV)	Cross Section (mb)
14.5	2060±700
14.8	2100±300
14.74	1591±143
14.4	1801±135
14.8	1378±206



TABLE III  
TERMS USED IN DATA ANALYSIS

Term	Value	Reference
T(Pr)	3.39±.01 min.	a
T(Ho)	40.8±.04 min.	this experiment
$\alpha$ (Ho)	4.752±.57	b
B(Pr)	47%	c
B(Ho)	15%	see page 18
f(Pr)	.72±.1	this experiment
f(Ho)	10.2±.2	this experiment
G(Pr)/G(Ho)	2	see page 16
(Pr)	1711±84 mb	see page 18
T(Cu)	9.9 min	d
B(Cu)	97.8%	d
f(Cu)	.72±.1	this experiment
G(Cu)/G(Ho)	2	see page 16
(Cu)	550 mb	e

APPENDIX B

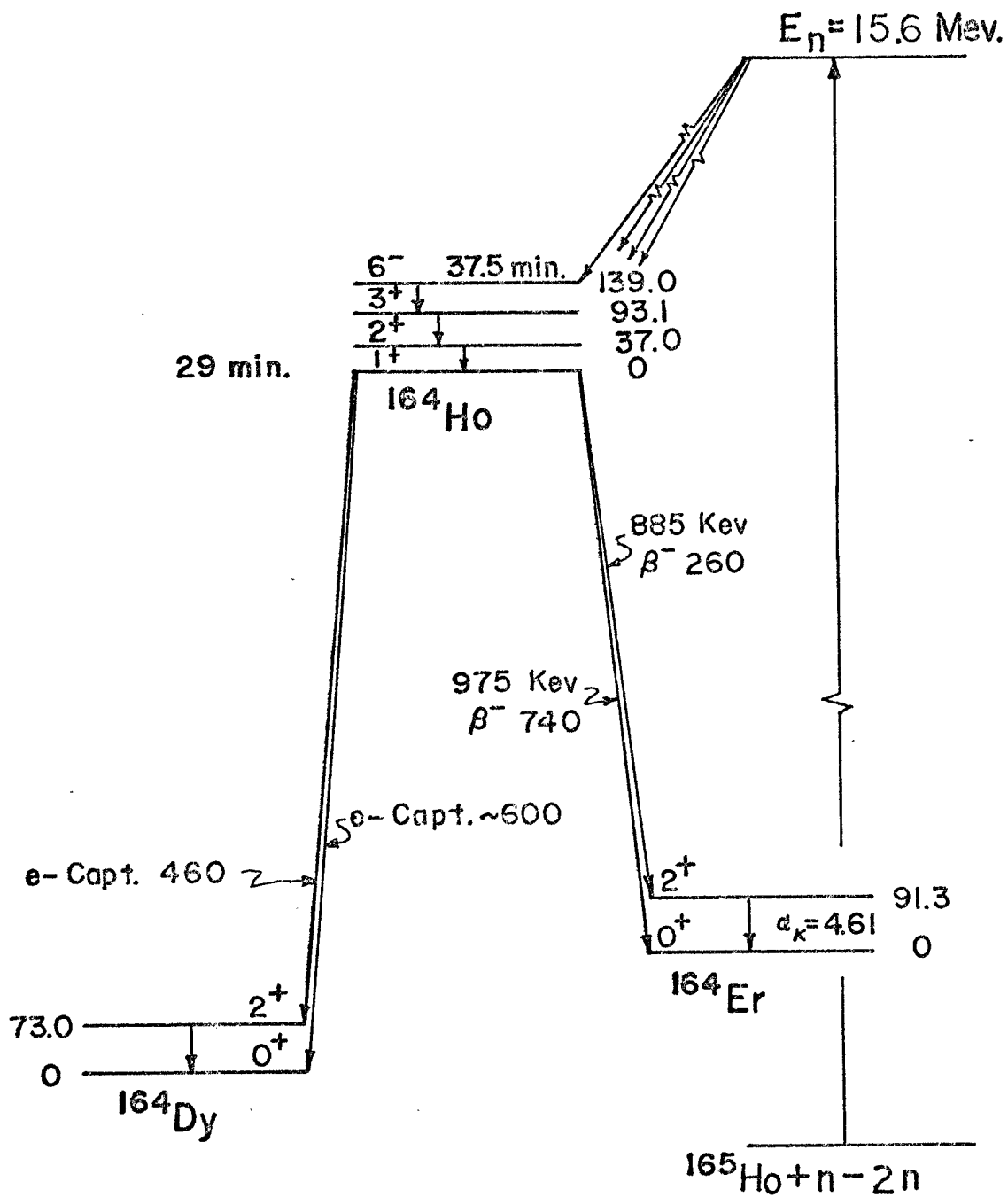


Fig. 1--Decay Scheme for  $^{164}\text{Ho}$

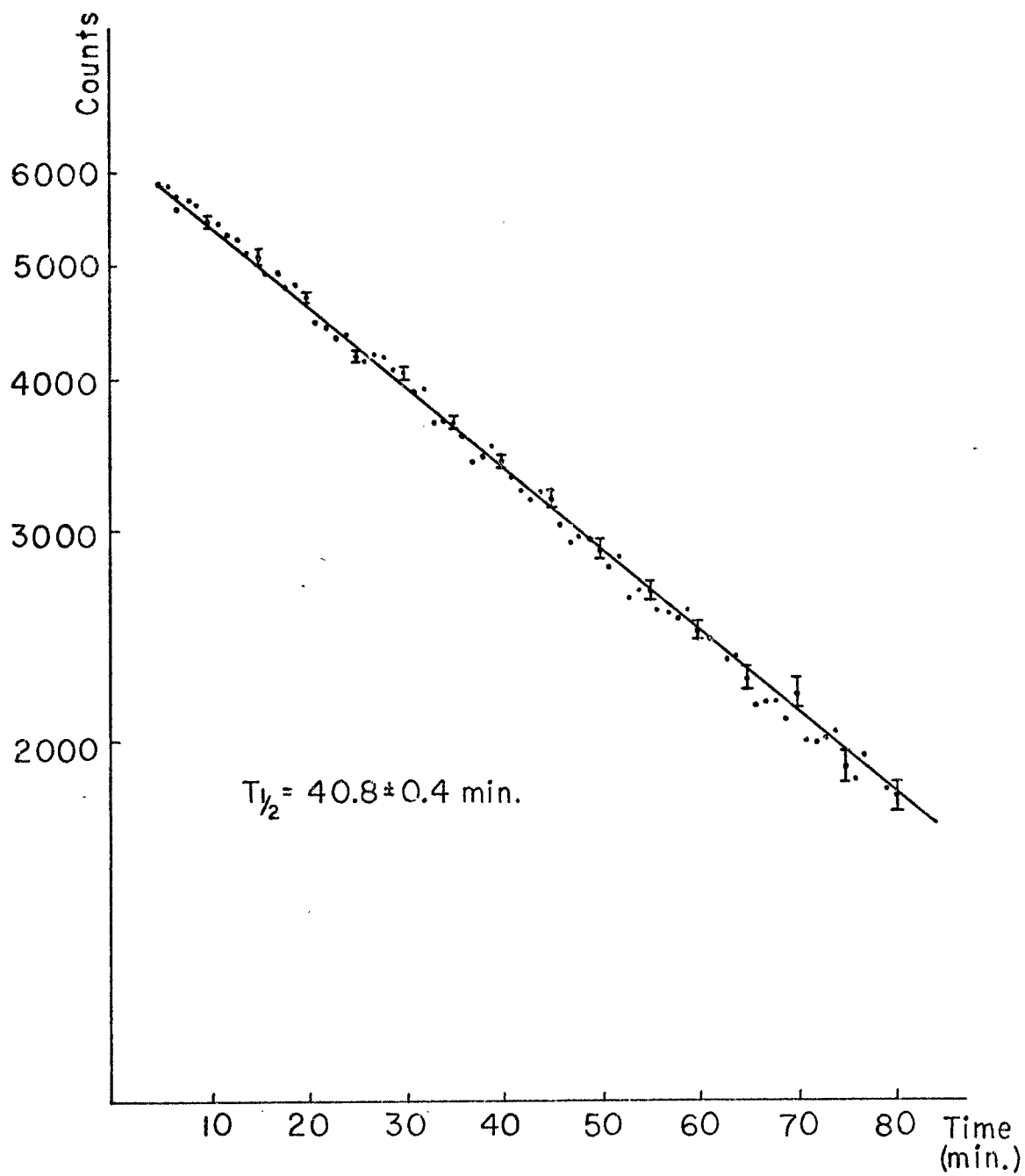


Fig. 2--Half-life Plot for  $^{164}\text{Ho}$

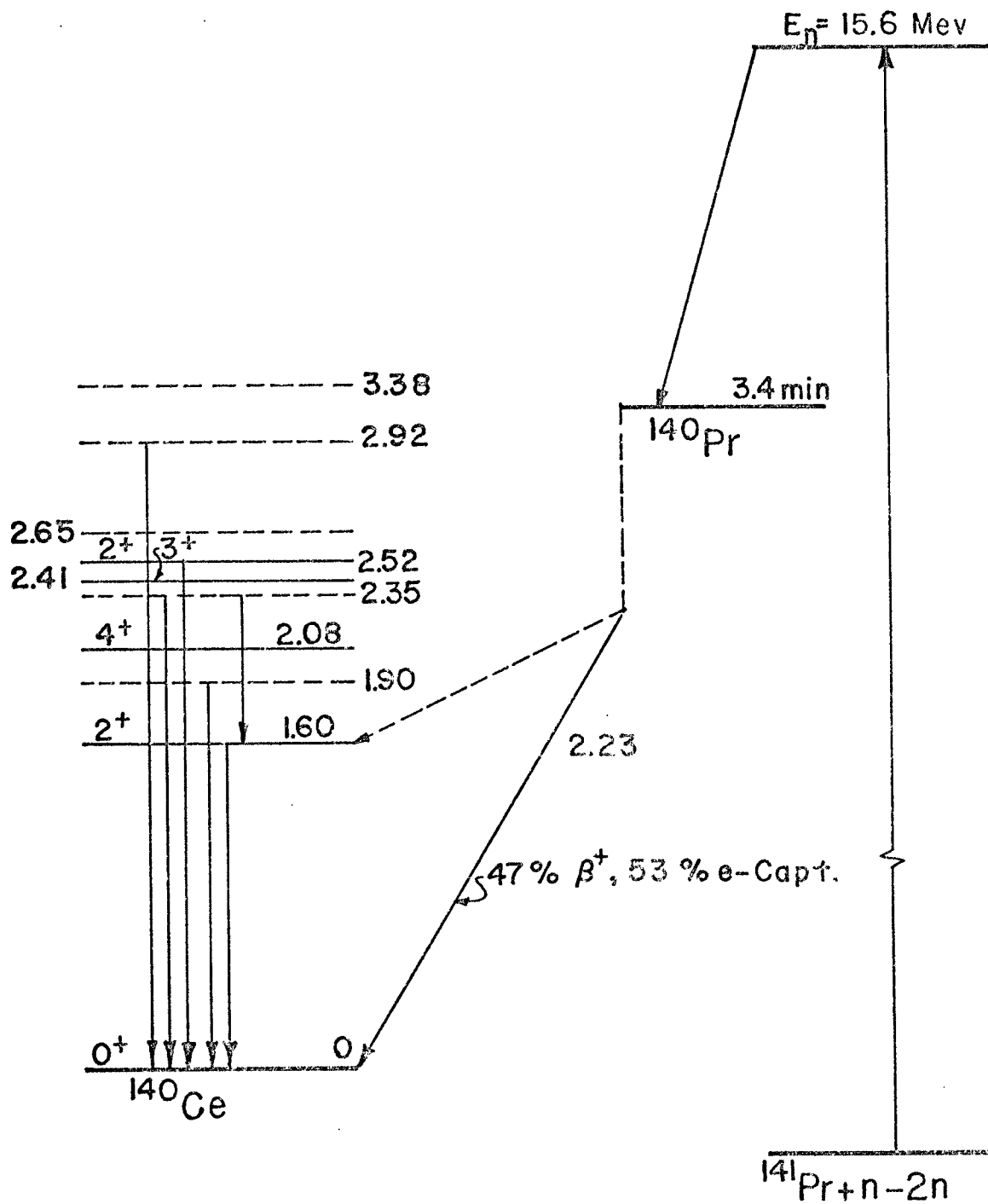


Fig. 3--Decay Scheme for  $^{140}\text{Pr}$

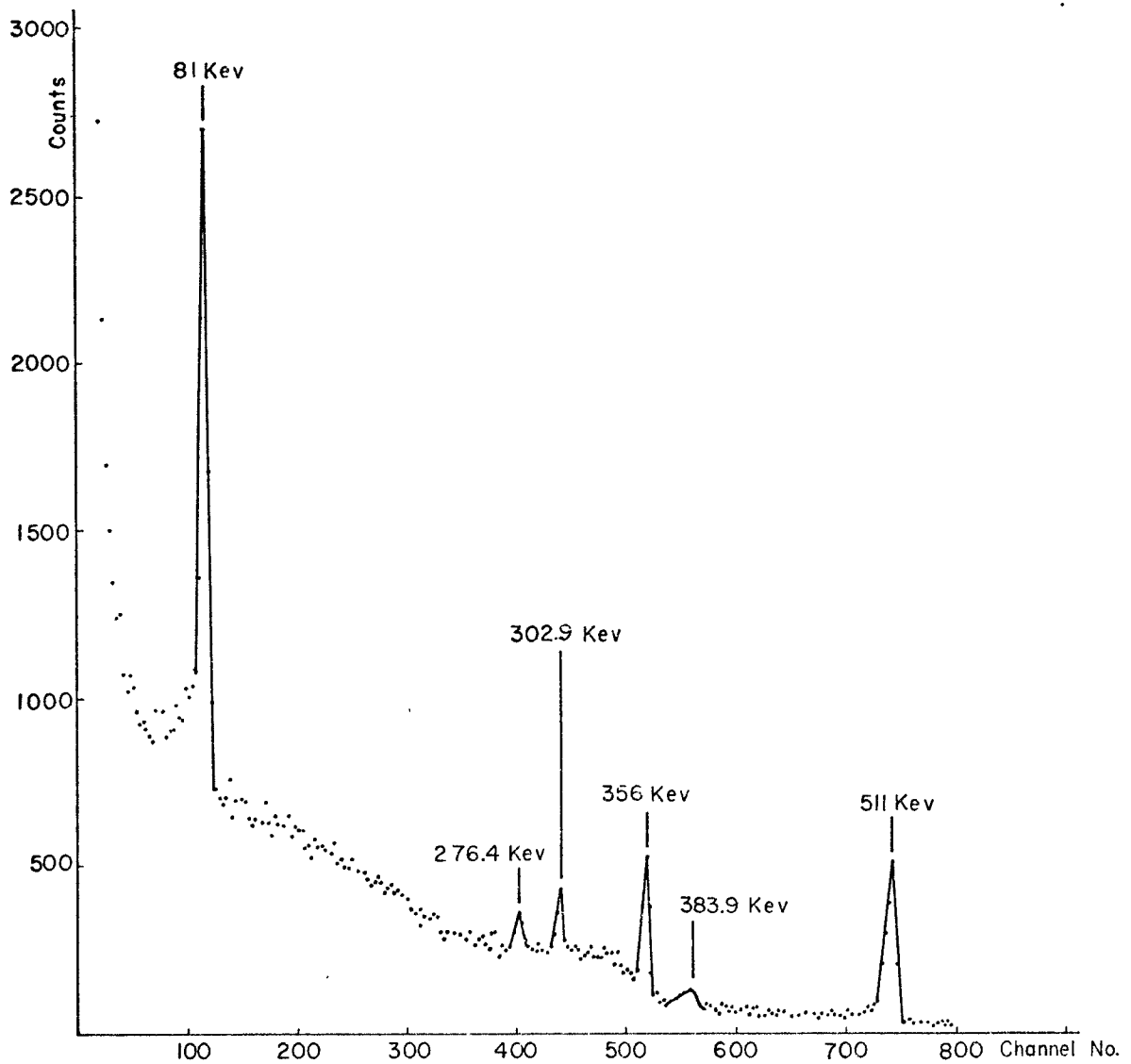
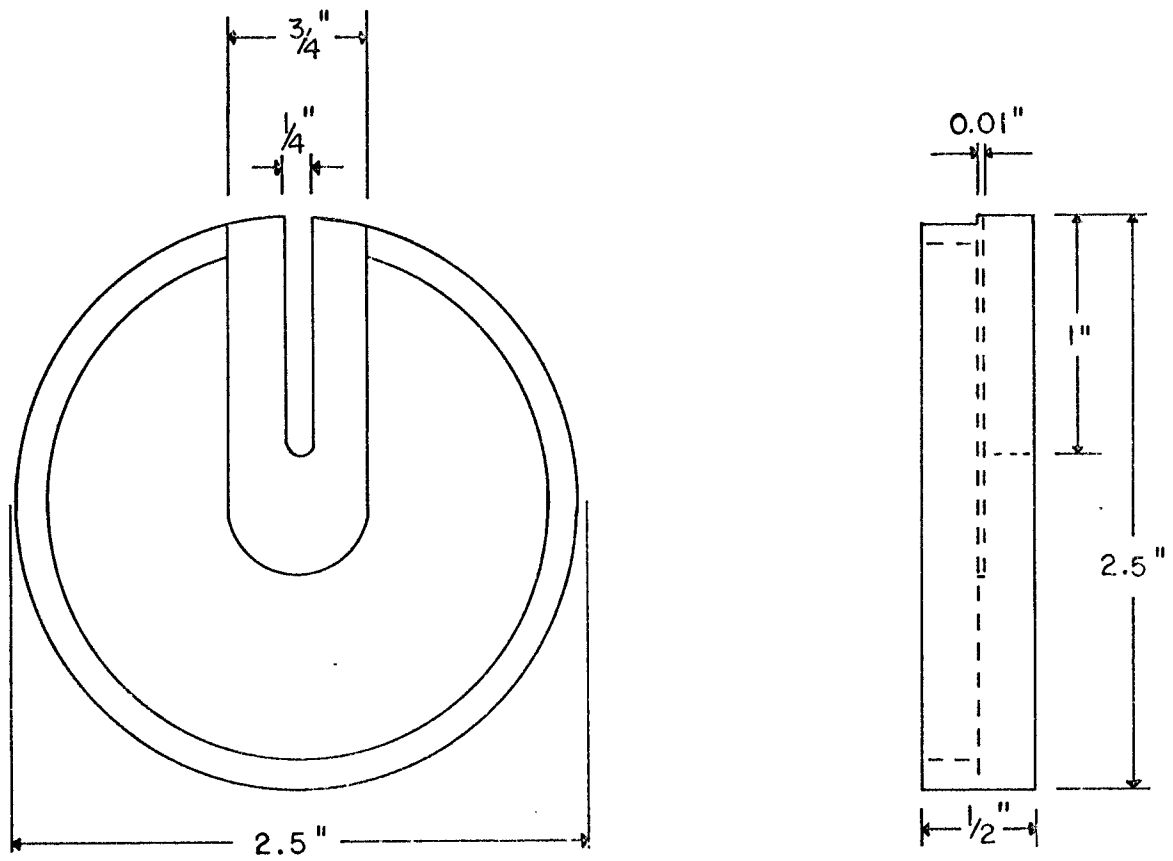


Fig. 4--Energy Calibration Spectrum



Front View

Side View

Fig. 5--Source Positioning Jig

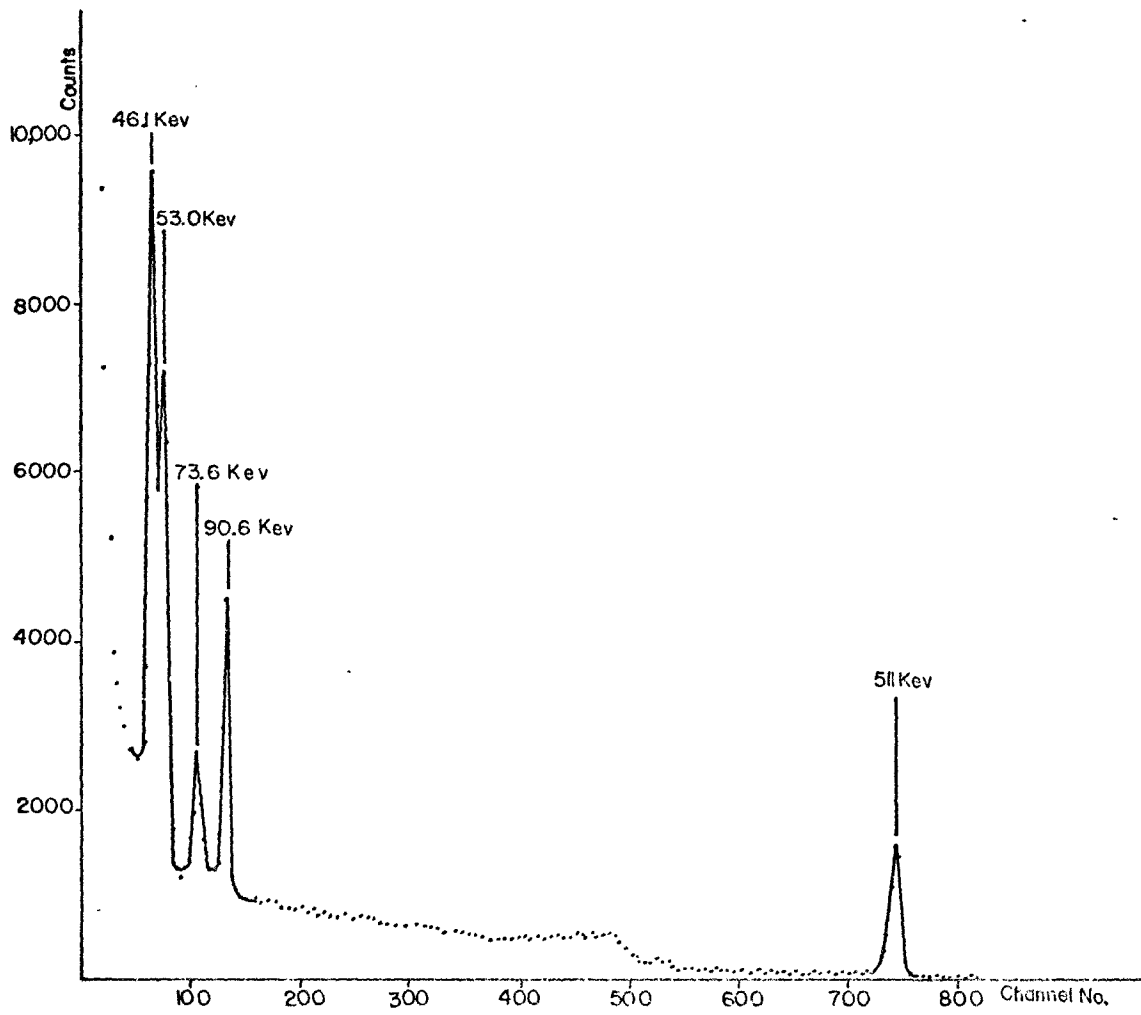


Fig. 6--Activation Spectrum of  $^{164}\text{Ho}$  and  $^{140}\text{Pr}$



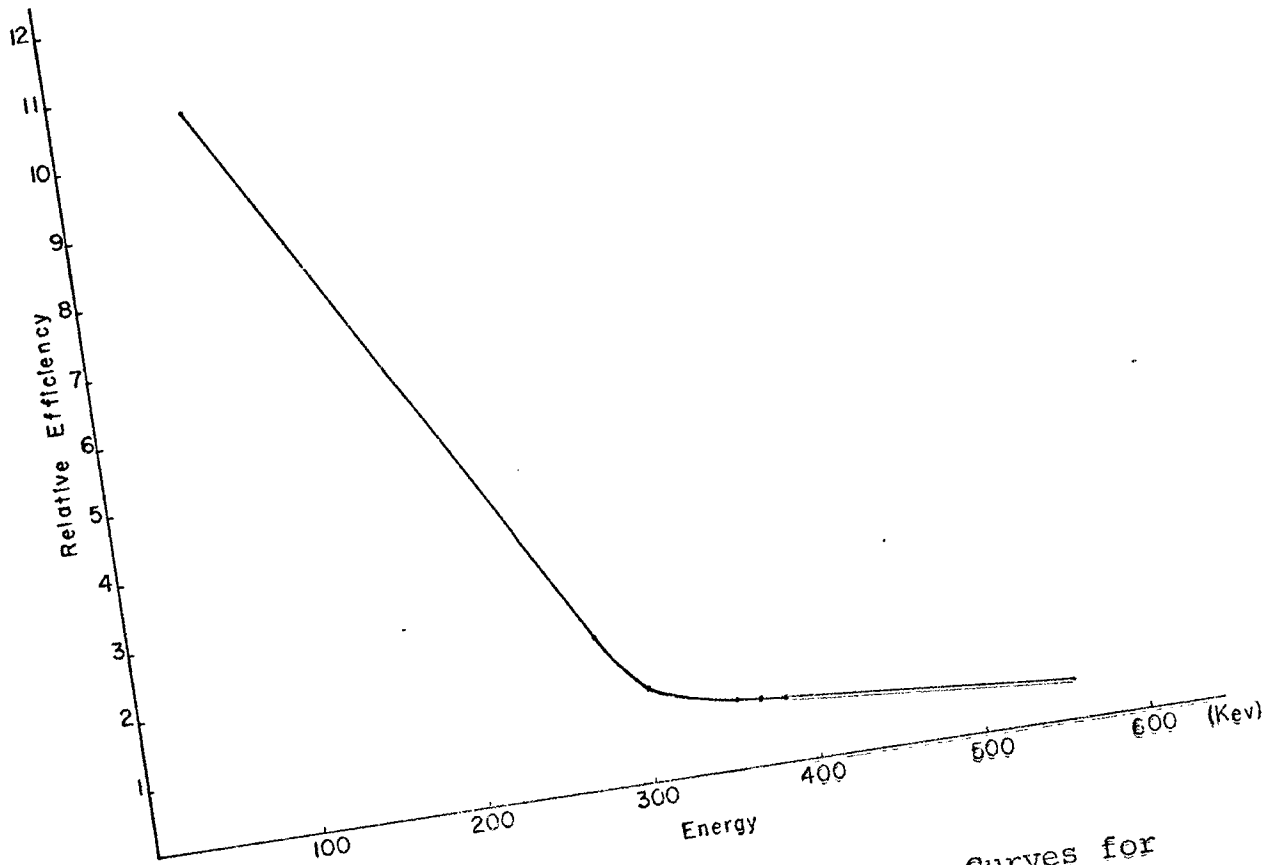


Fig. 7--Relative Efficiency vs Energy Curves for Ge(Li) Detector

## FOOTNOTES

1. C. S. Khurana and H. S. Hans, Nucl. Phys. 28, 560-69 (1961).
2. G. C. Bonazzola, P. Brovotto, E. Chiavassa, R. Spinoglio and A. Pasquarelli, Nucl. Phys. 51, 337-344 (1964).
3. B. Sethi and S. K. Mukherjee, Nucl. Phys. 85, 227-240 (1966).
4. H. O. Menlove, K. L. Coop and H. A. Grench, Phys. Rev. 163, No. 4, 1308-14 (1967).
5. Hugh N. Brown and Robert A. Becker, Phys. Rev. 96, No. 5, 1372-8 (1954).
6. M. H. Jorgensen, O. B. Nielsen and O. Skilbreid, Nucl. Phys. 84, 569-76 (1966).
7. Nuclear Data Group (ed.), Nuclear Data Sheets, Part 7, 1719 (1965), (no Vol. No.).
8. The Regional Nuclear Physics Laboratory is operated jointly by Southern Methodist University and North Texas State University. Facilities are located on each campus.
9. Jerry B. Marion and Betty Allen, A Tabulation of Neutron Energies From Various Charged Particle Reactions (Shell Development Co., Houston, 1955).
10. George H. Pepper, "Cs<sup>133</sup> (n, 2n) Cross-Section at 15.6 and 16.1 MeV," unpublished master's thesis, Department of Physics, North Texas State University, 1969, p.45.
11. KeveX-ray Systems, 1969 advertising manual distributed by Applied Spectroscopy Division, KeveX Corporation, Burlingame, California.
12. Nuclear Data Group (ed.), Nuclear Data Sheets 1, 521 (1965).
13. Nuclear Data Group (ed.), Nuclear Data Sheets, Part 6, 1284 (1965), (no Vol. No.).

14. Bob Lichtinger, Nuclear Diode Representative, personal communication.
15. Exact measurement not available from manufacturer.
16. Irving Kaplan, Nuclear Physics, (Addison-Wesley Publishing Co., Inc., Cambridge, 1956), p. 463.
17. Robley D. Evans, The Atomic Nucleus (McGraw-Hill Book Co., N. Y., 1955), Chap. 21, p. 628.
18. M. P. Ruffle, Nuclear Instruments and Methods 52, 354-6 (1967).
19. N. V. De Castro Faria and R. J. A. Levesque, Nuclear Instruments and Methods 46, 325-32 (1967).
20. D. P. Donnelly, H. W. Baer, J. J. Reidy and M. L. Wiedenbeck, Nuclear Instruments and Methods 57, 219-26 (1967).
21. Anne Ng, R. E. Wood, J. M. Palms, P. Venugopala Rao and R. W. Fink, Phys. Rev. 175, 1329-1338 (1968).
22. D. P. Donnelly, J. J. Reidy, and M. L. Wiedenbeck, Phys. Rev. 173, 1192-1201 (1968).
23. Thomas G. Ebrey and Peter R. Gray, Nucl. Phys. 61, 479-92 (1965).
24. S. Pearlstein, Nuclear Data, Section A, 3, No. 3 327-41 (1967).

FOOTNOTES FOR TABLE III

- a. Thomas G. Ebrey and Peter R. Gray, Nucl. Phys. 61, 479-92 (1965).
- b. Nuclear Data Group (ed.), Nuclear Data Sheets 1, 521 (1965).
- c. Nuclear Data Group (ed.), Nuclear Data Sheets, Part 6, 1284 (1965), (no Vol. No.).
- d. Nuclear Data Group (ed.), Nuclear Data Sheets, Part 2, 279 (1965), (no Vol. No.).
- e. Nuclear Data Group (ed.), Nuclear Data Sheets, 1, 171 (1965).

## BIBLIOGRAPHY

## Articles

- Bonazzola, G. C., Brovett, P., Chiavassa, E., Spinoglie, R., and Pasquarelli, A., "The Measurement by Activation of Cross Sections for 14.7 Mev Neutrons," Nucl. Phys. 51, (1964) 337-344.
- Bormann, M. (comp.), "Neutron Shell Effects in the (n, 2n) Cross Sections at 14 Mev," Nucl. Phys. 65, (1965) 257.
- Brown, Hugh N., and Becker, Robert A., "Radiations from Ho<sup>164</sup>," Phys. Rev. 96, No. 5 (1954) 1372-8.
- Donnelly, D. P., Baer, H. W., Reidy, J. J., and Wiedenbeck, M. L., "The Calibration of a Ge(Li) Gamma-Ray Spectrometer for Energy and Relative Intensity Measurement," Nuclear Instruments and Methods 57, (1967) 219-226.
- Donnelly, D. P., Reidy, J. J., and Wiedenbeck, M. L., "High-Resolution Gamma-Ray Spectroscopic Study of the Decay <sup>133</sup>Ba---<sup>133</sup>Cs," Phys. Rev. 173, No. 4 (1967) 1192-1201.
- Ebrey, Thomas G., and Gray, Peter R., "Precision Half-Life Measurements of Fourteen Positron-Emitting Nuclei," Nucl. Phys. 61, (1965) 479-492.
- Faria, N. V. De Castro, and Levesque, R. J. A., "Photopeak and Double-Escape Peak Efficiencies of Germanium Lithium Drift Detectors," Nuclear Instruments and Methods 46, (1967) 325-332.
- Jorgensen, M. H., Nielsen, O. B., and Skilbreid, O., "The Decay of 37.5 Min <sup>164</sup>Ho," Nucl. Phys. 84, (1966) 569-576.
- Khurana, C. S., and Hans, H. S., "Cross-Sections for (n, 2n) Reactions at 14.8 Mev," Nucl. Phys. 28, (1961) 560-569.
- Koenig, L. A., Mattauch, J. H. E., and Wapstra, A. H. (comps.), Nuclear Data Tables, Part 2, (1960), (no Vol. No.).

- Menlove, H. O., Coop, K. L., and Grench, H. A., "Activation Cross Sections for the  $F^{19}(n, 2n)F^{18}$ ,  $Na^{23}(n, 2n)Na^{22}$ ,  $Mn^{55}(n, 2n)Mn^{54}$ ,  $In^{115}(n, 2n)In^{114m}$ ,  $Ho^{165}(n, 2n)Ho^{164m}$ ,  $In^{115}(n, n')In^{115m}$ , and  $Al^{27}(n, \alpha)Na^{24}$  Reactions," *Phys. Rev.* **163**, No. 4 (1967) 1308-14.
- Ng, Ann, Wood, R. E., Palms, J. M. Rao, P. Venugopala, and Fink, R. W., "Gamma Rays from the Decay of  $^{75}Ge$  and  $^{77}Ge$ ," *Phys. Rev.* **176**, (1968) 219-26.
- Nuclear Data Group (ed.), *Nuclear Data Sheets*, Part 7, 1719, (1965), (no Vol. No.).
- Nuclear Data Group (ed.), *Nuclear Data Sheets*, Part 6, 1284, (1965), (no Vol. No.).
- Nuclear Data Group (ed.), *Nuclear Data Sheets*, 1, (1965) 521.
- Nuclear Data Group (ed.), *Nuclear Data Sheets* 1, (1965) 171.
- Pearlstein, S., "An Extended Table of Calculated (n, 2n) Cross Sections," *Nuclear Data*, Section A, 3, No. 3 (1967) 327-41.
- Ruffle, M. P., "The Geometrical Efficiency of a Parallel-Disc Source and Detector System," *Nuclear Instruments and Methods*, 52, (1967) 354-56.
- Sethi, B., and Mukherjee, S. K., "The Decay of  $^{164}Ho$ ," *Nucl. Phys.* **85**, (1966) 227-240.

#### Books

- Evans, Robley D., The Atomic Nucleus (McGraw-Hill Book Co., N. Y., 1955), Chap. 21, p. 628.
- Kaplan, Irving, Nuclear Physics (Addison-Wesley Publishing Co., Inc., Cambridge, 1956), p. 463.

#### Reports

- KeveX-ray Systems, advertising manual distributed by Applied Spectroscopy Division, KeveX Corporation, Burlingame, California, 1969.
- Marion, Jerry B., and Allen, Betty, A Tabulation of Neutron Energies From Various Charged Particle Reactions (Shell Development Co., Houston, 1955).

## Unpublished Materials

Lichtinger, Bob, Nuclear Diode Representative, personal communication, August 1968.

Pepper, George H., " $\text{Cs}^{133}$  (n, 2n) Cross-Section at 15.6 and 16.1 MeV," unpublished master's thesis, Department of Physics, North Texas State University, 1969.